

Supplementary Information

For

Nearly Lattice Matched All Wurtzite CdSe/ZnTe Type II Core-Shell Nanowires with Epitaxial Interfaces for Photovoltaics

Kai Wang, Satish C. Rai, Jason Marmon, Jiajun Chen, Kun Yao, Sarah Wozny,
Baobao Cao, Yanfa Yan, Yong Zhang,^{*} and Weilie Zhou^{*}

The supplement includes:

1. XRD of CdSe nanowires on silicon substrate;
2. Morphologies and structural analysis of ZnTe nanowires;
3. Atomic force microscopy (AFM) and additional photoluminescence measurements of CdSe nanowires and CdSe/ZnTe core/shell nanowires;
4. TEM analysis of ZnTe/CdSe core-shell nanowire;
5. The growth of CdSe nanowire array on mica substrate;
6. Electrical and photoresponse measurements for a bare CdSe nanowire device.

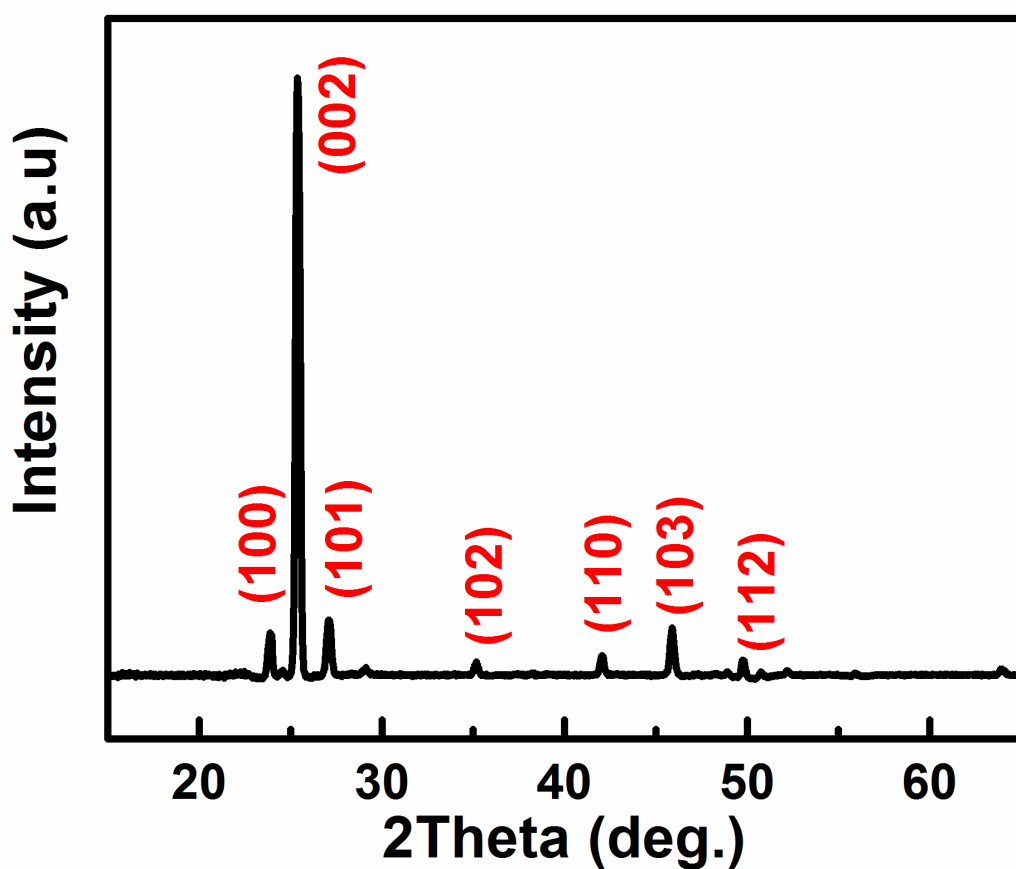


Figure S1. XRD pattern of CdSe nanowires collected on (100) silicon substrates.

XRD pattern of the CdSe nanowires grown on silicon substrate was shown in Figure S1. A very intense diffraction peak, (002), indicated that the CdSe product has a preferred *c*-axis orientation. Because of the presence of a relatively thicker CdSe bulk layer (as observed in SEM, Fig. 1(b)), we cannot solely attribute this to the *c*-axis growth direction of CdSe nanowires. In fact, similar to ZnO, CdSe naturally crystallizes in a wurtzite structure. This hexagonal structure prefers growth along the *c*-axis. Once the furnace is heated to a certain temperature, CdSe is evaporated and the high density vapor condensed on the silicon substrate in the first growth period, which led to a thin film oriented along the *c*-axis on silicon substrate. The thin film thickness was determined by the temperature gradient and the amount of the source vapor. Meanwhile, gold catalyzes initial nanowire growth using this oriented thin film as a seed layer. This could explain why the CdSe nanowires grown by this method were rigid. We also used XRD to obtain CdSe/ZnTe core-shell nanowire phase information. Compared to the CdSe nanowire XRD pattern in Figure S1, the core-shell pattern showed no additional diffraction peaks, presumably because of the high volume ratio of CdSe in the product and the identical phase structures and very similar lattice constants of CdSe and deposited ZnTe.

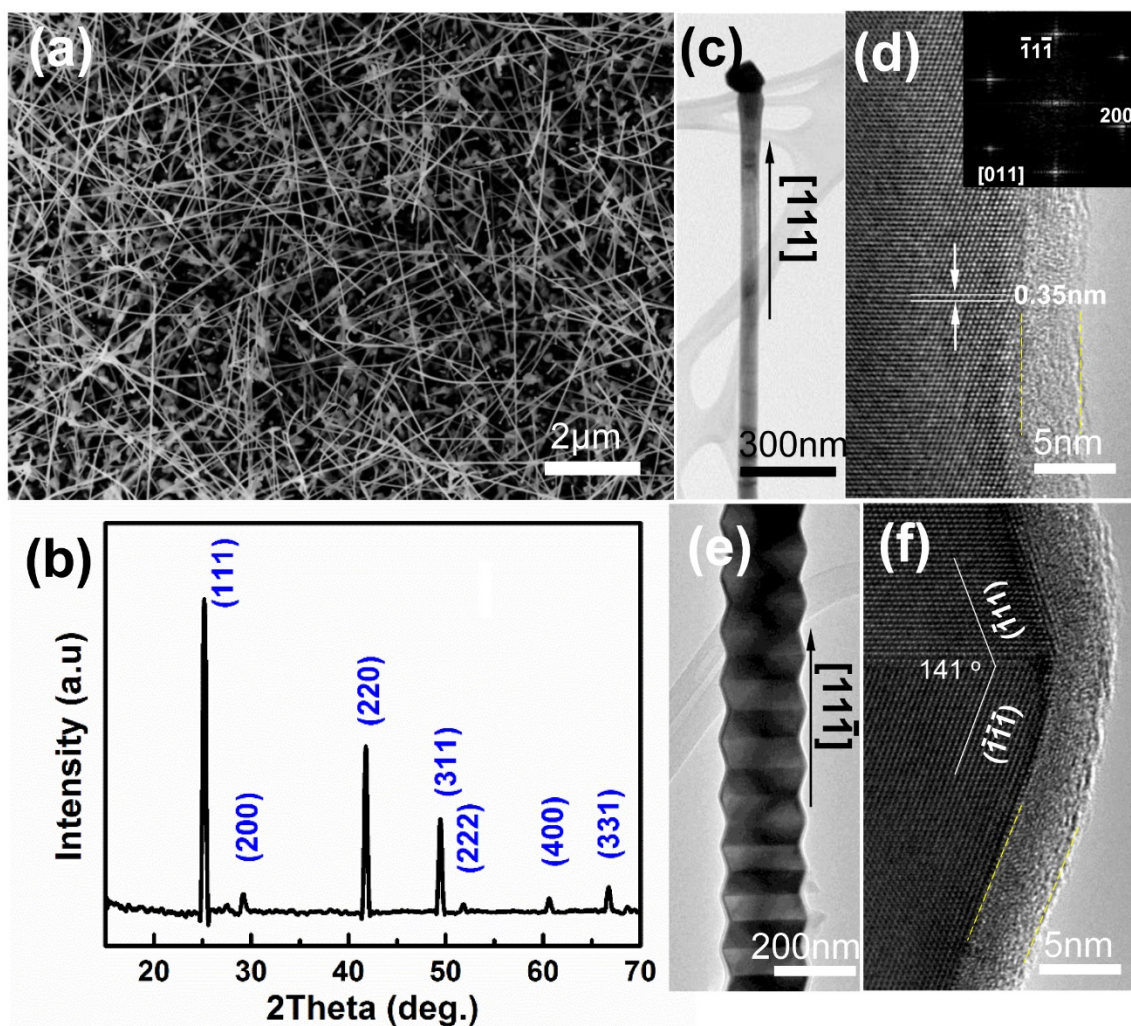


Figure S2. Structure analysis of ZnTe nanowires synthesized by thermal evaporation. (a) SEM image of ZnTe nanowires collected on silicon substrate. (b) XRD pattern of ZnTe nanowires synthesized by thermal evaporation. (c) and (e) Low magnification TEM images of ZnTe nanowires. (d) and (f) HRTEM images of ZnTe nanowire that correspond to the area marked in (c) and (e) respectively. The native oxide layer was highlighted by dashed, yellow line.

As shown in the SEM image in Fig. S2(a), ZnTe nanowires obtained by thermal evaporation had a diameter of 100 nm. Most of them exhibited a length on the order of tens of micrometers. Figure S2 (b) shows an XRD pattern for ZnTe nanowires on silicon substrate. All the diffraction peaks were indexed to a standard diffraction card (JCPDS No. 15-0746). Results indicated that ZnTe nanowires crystallize into zinc blende structures (space group F-43m (216)). Two representative ZnTe nanowire microstructures were obtained with low-magnification TEM Fig. S2(c) and (e). The nanowire in Fig. S2(c) is straight, while the one in Fig. S2(e) exhibits periodic twins along the entire length of the nanowire. Analysis of HRTEM and the corresponding SEAD pattern of the straight nanowire, as shown in Fig. S2(d), suggested the ZnTe nanowire is single crystalline, and its preferential growth direction along the [111] direction, and the lattice plane distance in this plane was measured to be 0.35 nm.

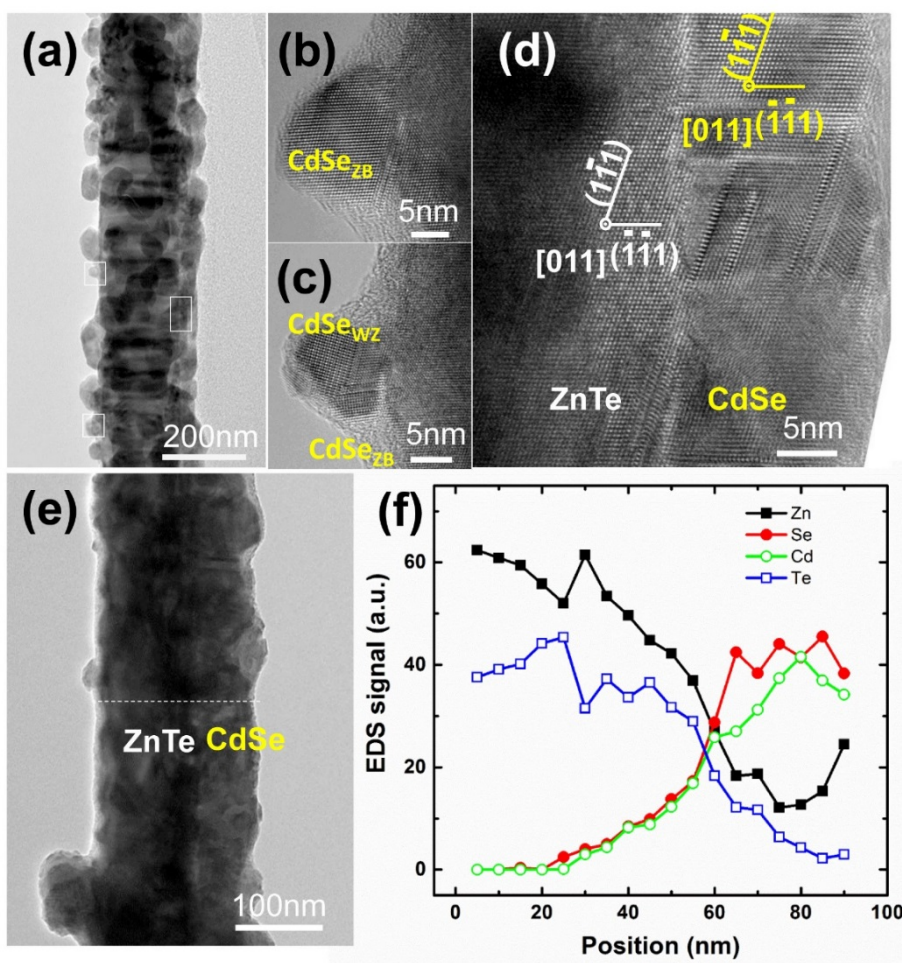


Figure S3. Structural analysis of ZnTe/CdSe nanowires. (a) Low magnification TEM images of ZnTe/CdSe nanowires. (b) and (c) HRTEM images of CdSe nanocrystals exhibiting epitaxial growth on the surface of ZnTe nanowires. (c) HRTEM image of a ZnTe/CdSe interface of nanowire where an epilayer of CdSe was observed. (e) Low magnification TEM image of a ZnTe/CdSe nanowire showing an inhomogeneous coating due to non-alignment of ZnTe nanowires. (f) Nanoprobe EDS result recorded along the dashed white line in (e).

In order to synthesize ZnTe/CdSe core-shell nanowires, the silicon substrate with as-grown ZnTe nanowires was transferred into home-made pulsed laser ablation system. A cold-pressed CdSe pellet was used as the ablation source. The distance between target and silicon substrate was measured as 40 mm. Before the laser beam was directed to the target, the system was pumped down to 30 mTorr and the temperature was increased to 450 °C. The laser fluence is similar to that for ZnTe deposition on CdSe nanowire. Low magnification TEM image in Fig. S3(a) revealed that several CdSe nanocrystals were attached on one side of a ZnTe nanowire, while the other side was covered by a continuous layer. HRTEM images of the nanocrystals, taken from the area marked with white in Fig. S3(a), were shown in Fig. S3(b) and (c). On the thick layer side, the CdSe layer crystallized in a zinc blende structure, despite a number of dislocations and other defects. It should be noted that most of the nanowires had inhomogeneous coatings. The primary reasons were random distributions of ZnTe nanowire and the ablated CdSe vapor blocked to form a conformal shell layer.

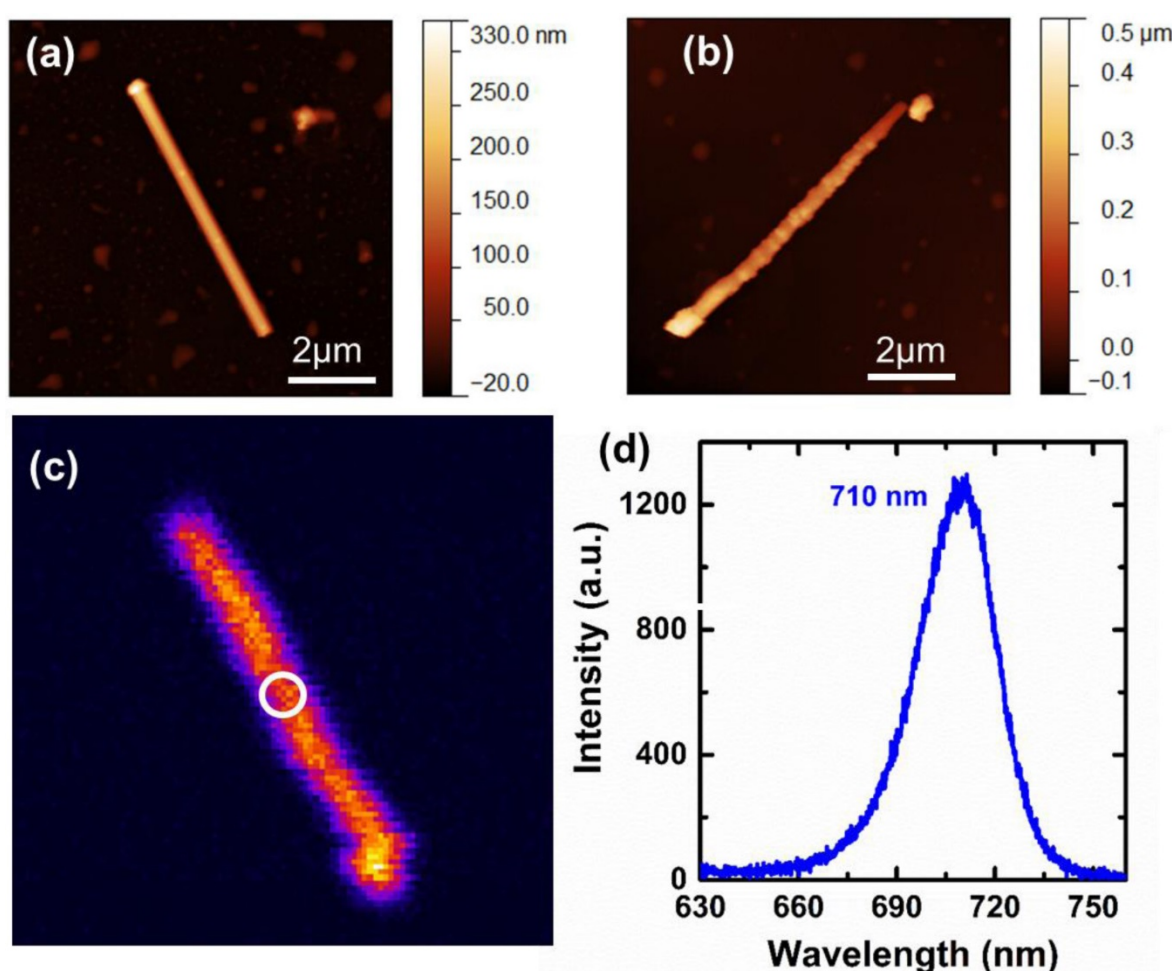


Figure S4. AFM and additional PL analysis of a CdSe nanowire and a CdSe/ZnTe core-shell nanowire. (a) and (b) AFM images of an individual CdSe nanowire and a CdSe/ZnTe core-shell nanowire. (c) PL image of a single CdSe nanowire. (d) PL spectrum of a CdSe nanowire collected from the area marked by circle in (c).

The morphologic information obtained in AFM, the catalyst on the tip and a smooth surface in particular, is in good agreement with previous electron microscope observations. An AFM image of a CdSe/ZnTe core-shell nanowire exhibited a rough surface, which is consistent with TEM observations. The spectrum in Fig. S4(d) has a corresponds to the area marked with a white circle in Fig. S4(c). The peak center at 710 nm corresponds to band emission of bulk CdSe. However, no photoluminescence was recorded for the CdSe/ZnTe core-shell nanowires. The reason may be due to the larger ZnTe shell thickness compared to the one in the main document.

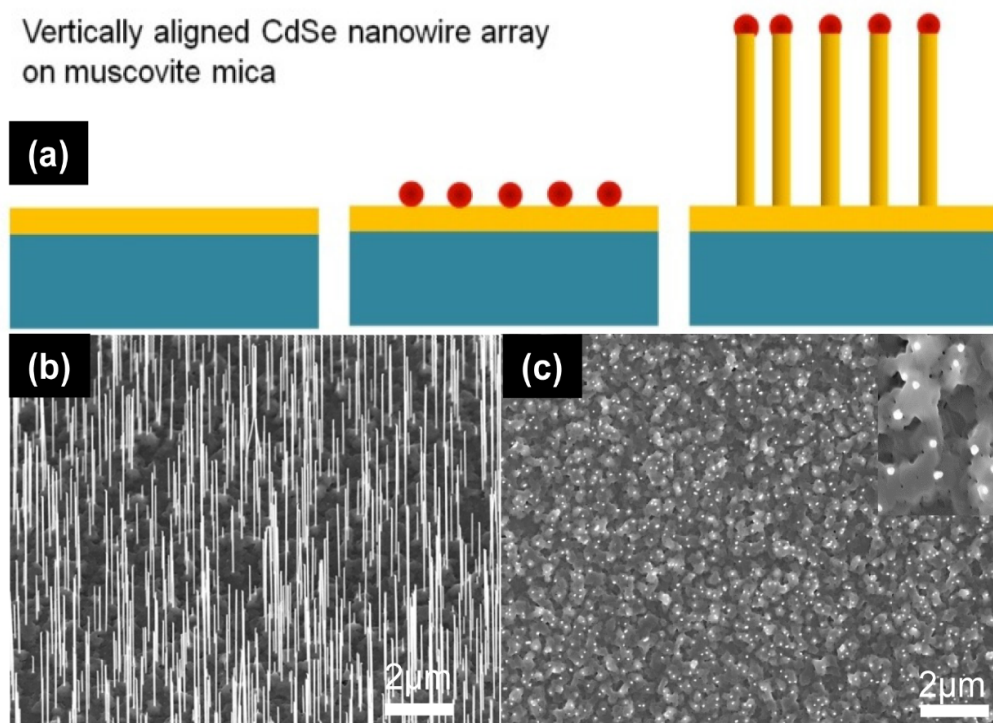


Figure S5. The growth of CdSe nanowire array. (a) Schematic of CdSe nanowire array growth on muscovite mica by using CdSe thin film and gold as barrier layer and catalysts. (b) and (c) tilted and top-view SEM images of CdSe nanowire array on CdSe thin film/mica substrates, demonstrating the vertically-aligned morphology. Inset in panel (c) shows an enlarged top-view SEM images of the nanowire array. The (0001) oriented CdSe epilayer was epitaxially grown on mica substrate via van der Waals epitaxy and acts as charge collecting layer in optotronic devices. Technically, the diameter and density of nanowires are determined by the catalyst size and distribution.

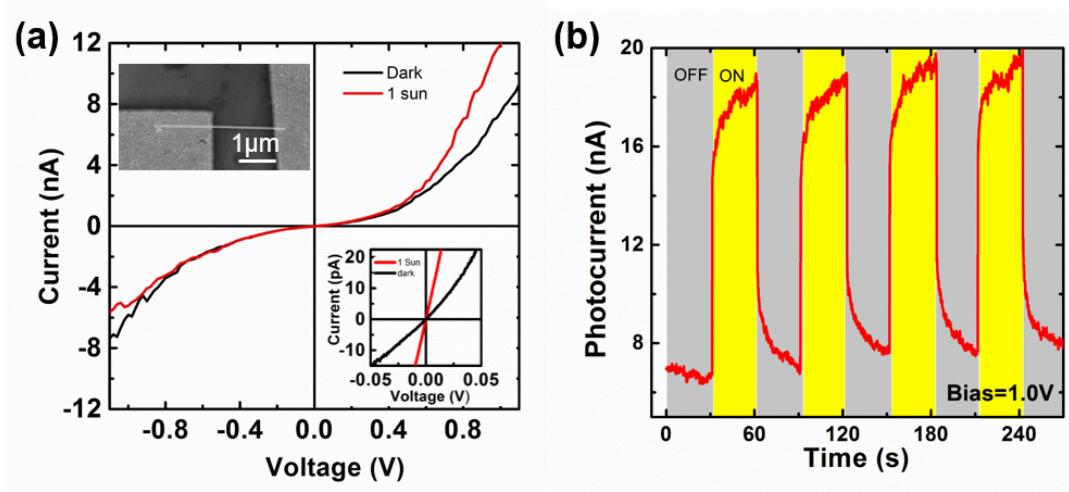


Figure S6. Electrical characterization of a single CdSe nanowire nanodevice.

(a) Current-voltage (I - V) characteristic for a bare CdSe nanowire device under global AM 1.5 illumination and dark current. The device is consisting of a pure CdSe nanowire bridged across a pair of gold electrodes. An SEM image of the corresponding device is shown in the upper inset, while the lower inset contains the I - V curve in lower voltage range. (b) Photoresponse of the nanowire device measured with a 1.0 V bias.